The Air Pressure on a Cone Moving at High Speeds. I.

G. I. TAYLOR and J. W. MACCOLL,

Proceedings of the Royal Society of London.
Series A, Vol. 139, No. 838 (Feb. 1, 1933), pp. 278-297

§1. Introduction and Summary.

When a body moves through air at a uniform speed greater than that of sound, a shock wave is formed which remains fixed relative to the body. This wave is situated on a surface where a very abrupt change in density and velocity occurs. It can be seen as a sharp line in photographs of bullets in flight. In front of this surface the air is stationary, behind it there is a continuous field of fluid flow which may contain further shock waves. The nature of these shock waves is well known and the equations which govern their propagation were first obtained by Rankine.[1] The work of Rankine, however, seems to have escaped the notice of subsequent writers and it was not till some years later that they were rediscovered by Hugoniot[2] to whom they are usually attributed. Rankine's equations give the relationship between the conditions in front and behind a plane shock wave. They connect the ratio of the density in front and behind the wave with the components of velocity normal to the wave. They have been applied by Meyer[3] to find the flow in the neighbourhood of an inclined plane or wedge moving at high speeds.

Meyer begins with a plane shock wave reduced to rest by giving the whole field a suitable velocity perpendicular to its plane. He then gives the whole field a velocity parallel to the wave front. The system is then a steady one, the shock wave remaining at rest, but the direction of motion of the air, which is now oblique to the wave, suffers an abrupt change at the wave front. By combining two such shock waves intersecting at a point, but not continuing beyond the intersection, a system can be devised in which all the air on one side of the pair of waves is moving with a uniform velocity. The air which passes through one wave is deflected, say, upwards, while that which passes through the other is deflected downwards. This system can evidently be bounded by a solid wedge, the faces of which are parallel to the two parts of the deflected air stream.

Meyer exhibited this solution of the flow near a **wedge** moving at high speed by means of a series of curves showing the relationships between the pressure, speeds and angle of the wedge. His equations were reproduced by Ackeret[4]

---

1 'Phil. Trans.,' vol. 160, p. 277 (1870).
2 'Ec. polyt., Paris,' vols. 57-59, p. 1 (1887-1889).
3 'Mitt. ForschArb. Ingenieurw. V.D.I.,' No. 62 (1908).
4 "Gasdynamik," 'Handbuch der Physik,' vol. 7, chap.5 (1927).

who added a photograph of the flow in the neighbourhood of a wedge showing that Meyer's regime does in fact occur. The solution has certain limitations which are obvious from an inspection of Meyer's curves. These limitations have been treated independently and in greater detail by Bourquard.[5]

When the wedge is replaced by a **cone** no solution exactly similar to Meyer's can be obtained, because after passing obliquely through a conical shock wave the air cannot continue to flow in the direction into which it was first deflected. The pressure behind the shock wave, therefore, cannot be uniform, as it is in the case of the wedge. On the other hand, it turns out that an **irrotational solution** of the flow in the neighbourhood of a solid cone can be found such that the pressure, velocity and density of the stream is constant over coaxial cones passing through the same vertex.

If a conical shock wave is capable of changing the air from a state of uniform motion parallel to the axis of the cone to a condition which satisfies the irrotational solution mentioned above, then the system so constructed is a possible solution of the problem of flow at high speeds past a cone. That such solutions can be found has been suggested by Busemann,[6] who gave a graphical method for obtaining them. In his very short note on the subject no details or results are given so that we cannot make a comparison between his work and ours. It is clear, however, that his graphical method is capable of doing what he claims for it, though we have been unable to find any account of further developments on those lines.

In the present paper it is shown that under certain conditions the conical regime is possible and the **complete solution** is worked out by numerical integration, for three cones of semi-vertical angles 10°, 20° and 30°.

The calculated pressures at the surface of the cone are compared with observations of pressure made in a high speed wind channel and excellent **agreement** is found. In one case, that of the 60° cone (i.e., 30° semi-vertical angle), further comparisons are made with photographs of bullets in flight, and it is found that the **limitation** indicated by mathematical analysis that in this case the conical regime is possible only when the speed is greater than 1.46a, a being the speed of sound, corresponds with the condition observed in bullet photographs that at speeds less than 1.46a the shock wave leaves the conical nose of the bullet and remains **detached** a short distance ahead of it. At speeds higher than 1.46a the measured semi-vertical angle of the conical shock wave is in perfect agreement with that predicted by theory.

---

[5] Bourquard, 'Mémor. Artill.f rançaise,'vol. 11, p. 135 (1932).

[6] Busemann, 'Z. angew. Math. Mech.' vol. 9, p. 496 (1929).

As might be expected, the shock wave remains in contact with the point of the cone at lower speeds than it does with the leading edge of a wedge of the same angle.

After a greater part of this work was complete a note by Bourquard[7] appeared in the 'Comptes Rendus' from which it is clear that he is working on similar lines, but as no details are yet available we have not been able to compare our results with his.

On the other hand, we have been able to compare our complete solution with an approximate one applicable to any thin spindle-shaped body (including the cone of small vertical angle) which has recently been given by v. Karman and Moore.[8] Good agreement within a limited range is found in the case of the 20° cone, i.e., the cone with a semi-vertical angle of 10°. Considerable divergence is found in the case of the 40° cone and as might be expected there is still greater divergence in the case of the 60° cone. It was the knowledge that Professor v. Karman was working on these lines that led us, a year ago, to develop the complete solution for the cone, with a view to finding how far such approximations can be applied to cases where the disturbance is not very small.

§2. Hydrodynamical Equations.

List of Symbols.-The notation adopted is shown in fig. 1. r, θ are polar co-ordinates, $\theta = 0$ being the axis of a solid cone whose vertical angle is $2\theta_s$.

θ_w is the semi-vertical angle of a conical shock wave.

(u, v) are the radial and tangential components of velocity, and q is the velocity of the stream, to that $q^2 = u^2 + v^2$.

U is the velocity of the undisturbed stream, approaching the cone, or in the case of a conical headed projectile the velocity of the projectile.

(u_s, 0) are the components of velocity at the surface of the solid cone.

p, ρ are the pressure and density of air at any point behind the shock wave.

p_1, ρ_1, a are the pressure, density and velocity of sound in the undisturbed stream.

γ is the ratio of the specific heats so that $a^2 = \frac{\gamma p_1}{\rho_1}$. The value $\gamma = 1.405$ is used throughout the calculations.

p_2, ρ_2, p_s, ρ_s are the pressure and density immediately behind the shock wave and at the surface of the cone.

---

[7] 'C. R. Acad. Sci. Paris,' vol. 194, p. 846 (March 7, 1932).

[8] 'Trans. Amer. Soc. Mech. Eng.' (1932).

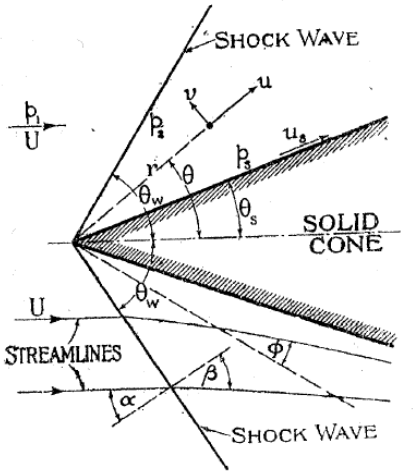

FIG. 1.

p_0, ρ_0 are the pressure and density of air at rest in a reservoir, which could attain the condition p_1, ρ_1, U by flowing in a steady stream under adiabatic conditions. Evidently $p_0 \rho_0^{-\gamma} = p_1 \rho_1^{-\gamma}$.

p_3, ρ_3 are the pressure and density of air at rest corresponding with the conditions behind the shock wave, so that $p_3 \rho_3^{-\gamma} = p_2 \rho_2^{-\gamma}$.

c_1, c are the velocities at which air at rest in the states (p_0, ρ_0) and (p_3, ρ_3) would flow into a vacuum under adiabatic conditions.

a* is the local speed of sound at any point behind the shock wave. The local speed of sound is the speed at which sound waves would be propagated through air in the condition (p, ρ); it is *not* the speed at which sound would be propagated relative to the cone.

α is the angle between the normal to the shock wave and the streamlines in front of it. These are parallel to the axis of the cone so that $\theta_w = \pi/2 - \alpha$.

β is the angle between the normal to the shock wave and the streamlines immediately behind the shock wave.

ϕ is the angle between the streamline at any point and the radius vector from the point of the cone.

The following symbols are used in conformity with Meyer and Ackeret's notation in order to reduce the formulae to non-dimensional forms:-

$$\begin{cases} x = p_2 / p_0 \\ y = p_1 / p_0 \\ z = p_3 / p_0 \end{cases}.$$

Irrotational Motion.-A solution of the equations of fluid flow near a solid cone will be sought in which all the variables, such as pressure, density and velocity, are functions of θ only. In this case the flow must be **irrotational** and the condition for irrotational flow is

$$\frac{\partial u}{\partial \theta} - v = 0 . \qquad (1)$$

The condition of **continuity** is

$$\frac{\partial}{\partial r}(\rho u r^2 \sin\theta) + \frac{\partial}{\partial \theta}(\rho v r \sin\theta) = 0 ,$$

and, since $\frac{\partial u}{\partial r} = 0$, this is

$$2\rho u \sin\theta + \frac{d}{d\theta}(\rho v \sin\theta) = 0 . \qquad (2)$$

$$-\frac{1}{c}\frac{d^2u}{d\theta^2} = \frac{L}{M}$$
$$L = \frac{1}{c^3}\left\{(\gamma-1)(c^2-u^2-v^2)(u+\frac{1}{2}v\cdot\cot\theta) - uv^2\right\}$$
$$M = \frac{1}{c^2}\left\{\frac{\gamma-1}{2}(c^2-u^2) - \frac{\gamma+1}{2}v^2\right\}$$

Hence, combining (1) and (2),

$$-\frac{v}{\rho}\cdot\frac{d\rho}{d\theta} = \frac{d^2u}{d\theta^2} + \cot\theta\cdot\frac{du}{d\theta} + 2u . \qquad (3)$$

The **adiabatic relationship** between pressure and density is $\frac{p}{p_3} = \left(\frac{\rho}{\rho_3}\right)^{\gamma}$ so that **Bernouilli's equation** is

$$\frac{\gamma p_3 \rho^{\gamma-1}}{(\gamma-1)\rho_3{}^{\gamma}} + \frac{1}{2}(u^2+v^2) = \text{constant} = \frac{1}{2}c^2 = \frac{\gamma}{\gamma-1}\frac{p_3}{\rho_3} , \qquad (4)$$

where *c* is the velocity which the gas would attain if allowed to flow in steady motion into a vacuum and p_3 , ρ_3 are the pressure and density at points where the velocity is zero.

Differentiating (4) with respect to θ and substituting $\frac{du}{d\theta}$ for *v*

$$\frac{\gamma p_3}{\rho_3{}^{\gamma}}\cdot\rho^{-\gamma}\cdot\frac{d\rho}{\rho d\theta} + u\frac{du}{d\theta} + \frac{du}{d\theta}\frac{d^2u}{d\theta^2} = 0 , \qquad (5)$$

and substituting for $\frac{1}{\rho}\frac{d\rho}{d\theta}$ from (3), (5) becomes

$$u\frac{du}{d\theta} + \frac{du}{d\theta}\frac{d^2u}{d\theta^2} = \frac{\gamma p_3}{\rho_3{}^{\gamma}}\cdot\rho^{-\gamma-1}\cdot\left(\frac{\frac{d^2u}{d\theta^2} + \cot\theta\frac{du}{d\theta} + 2u}{\frac{du}{d\theta}}\right), \qquad (6)$$

and substituting for $\rho^{\gamma-1}$ from (4), (6) becomes

$$\frac{du}{d\theta}\left(u\frac{du}{d\theta} + \frac{du}{d\theta}\frac{d^2u}{d\theta^2}\right) = \frac{\gamma-1}{2}\left\{c^2 - u^2 - \left(\frac{du}{d\theta}\right)^2\right\}\left\{\frac{d^2u}{d\theta^2} + \cot\theta\frac{du}{d\theta} + 2u\right\} .$$

(7)

This equation may be re-arranged into the more convenient form

$$\frac{1}{c}\frac{d^2u}{d\theta^2}\left\{\frac{\gamma+1}{2c^2}\left(\frac{du}{d\theta}\right)^2-\frac{\gamma-1}{2}\left(1-\frac{u^2}{c^2}\right)\right\}$$
$$=(\gamma-1)\frac{u}{c}\left(1-\frac{u^2}{c^2}\right)+\frac{\gamma-1}{2c}\left(1-\frac{u^2}{c^2}\right)\cot\theta\frac{du}{d\theta}-\frac{\gamma u}{c^3}\left(\frac{du}{d\theta}\right)^2-\frac{\gamma-1}{2c^3}\cot\theta\left(\frac{du}{d\theta}\right)^3 \tag{8}$$

This equation determines the motion when any initial values of *u*, *v* and θ are given.

To determine the pressure at any point when the solution of (8) is known (4) may be used. This may be written in the form

$$\frac{p}{p_3}=\left(1-\frac{u^2}{c^2}-\frac{v^2}{c^2}\right)^{\gamma/(\gamma-1)}. \tag{9}$$

The pressure, velocity and direction of motion of the flow behind the shock wave are given by (8) and (9).

In front of the shock wave the velocity is uniform and equal to *U* while the pressure is p_1 so that the pressure equation equivalent to (9) applicable to that region is

$$y=\left(1-\frac{U^2}{{c_1}^2}\right)^{\gamma/(\gamma-1)}, \tag{10A}$$

where *y* is written for $\frac{p_1}{p_0}$, and p_0 is the pressure in a reservoir from which air could flow with velocity *U*, pressure p_1 and density ρ_1. c_1 is the velocity at which gas at pressure p_0 and density ρ_0 discharges into a vacuum.

It is more usual to express velocities in terms of *a*, the velocity of sound in the undisturbed air. To find $\frac{c_1}{a}$, equation (4) may be applied to the region in front of the shock wave, thus

$${c_1}^2=\frac{2\gamma}{\gamma-1}\frac{p_0}{\rho_0} \quad \text{and} \quad a^2=\gamma\frac{p_1}{\rho_1},$$

so that

$$\frac{{c_1}^2}{a^2}=\frac{2}{\gamma-1}\frac{p_0}{p_1}\frac{\rho_1}{\rho_0}=\frac{2}{\gamma-1}\left(\frac{1}{y}\right)^{1-\frac{1}{\gamma}}.$$

Substituting this expression in (10A),

$$\frac{U^2}{a^2}=\frac{2}{\gamma-1}(y^{-(\gamma-1)/\gamma}-1). \tag{10B}$$

§3. Numerical Integration of Equation (8).

It is hardly to be expected that solutions of (8) could be found in finite terms, but on the other hand (8) is in a form suitable for numerical calculation. At the solid surface $\theta = \theta_s$ and $v = \frac{du}{d\theta} = 0$ so that the initial value of $\frac{d^2u}{d\theta^2}$ can be found. It is equal to $-2u_s$.[9] If $\delta\theta$ is a small increment in θ, the value of $\frac{du}{d\theta}$ at $\theta = \theta_s + \delta\theta$ is $-2u_s \cdot \delta\theta$ and the value of $\frac{u}{c}$ is

$$\frac{u_s}{c} + \frac{1}{2}\left(-\frac{2u_s}{c}\right)\cdot\delta\theta^2 .$$

These values of $\frac{u}{c}$ and $\frac{1}{c}\frac{du}{d\theta}$ may now be inserted in (8) to find the value of $\frac{1}{c}\frac{d^2u}{d\theta^2}$ at $\theta = \theta_s + \delta\theta$, and this value may again be used to find the values of $\frac{u}{c}$ and $\frac{1}{c}\frac{du}{d\theta}$ at $\theta = \theta_s + 2\delta\theta$. This method of step-by-step calculation will give the solution of (8) when any given initial values of $\frac{u_s}{c}$ and θ_s, are chosen.

$$\left.\frac{v}{c}\right|_i = \frac{1}{c}\cdot\left.\frac{du}{d\theta}\right|_i = \frac{1}{c}\left\{ v|_{i-1} + \delta\theta\cdot\left.\frac{d^2u}{d\theta^2}\right|_{i-1}\right\}$$

$$\left.\frac{u}{c}\right|_i = \frac{1}{c}\left\{u|_{i-1} + \delta\theta\cdot[v_M]\right\}$$

$$v_M = \frac{1}{2}\left(v|_i + v|_{i-1}\right)$$

$$-\frac{1}{c}\cdot\frac{d^2u}{d\theta^2} = \frac{L}{M}$$

The **accuracy** of the method will depend on the magnitude of $\delta\theta$. In some cases sufficient accuracy can be obtained by taking steps of three degrees, while in others smaller intervals must be taken. In some cases it was necessary to proceed by steps as small as 0.5°. The accuracy of the method in any given case may be judged by repeating the process using steps only half as great as those first taken. If there is no change in the results to the order of accuracy required, the steps may be considered as so small that no further diminution in $\delta\theta$ would produce any appreciable change in the result.

To illustrate the method, the complete calculation is given in Table I, for one case, namely, that of a 60° cone ($\theta_s = 30°$) when $\frac{u_s}{c} = 0.35$.

In this case it was found that the interval $\delta\theta = 3°$ was small enough to give the required accuracy. The calculation is carried from $\theta = 30°$ to $\theta = 69°$ and the variations in *u*/*c*, *v*/*c* with θ are shown in the curves marked $\frac{u_s}{c} = 0.35$ in fig. 2. It will be seen that as θ increases *u*/*c* and *v*/*c* decrease. The values of

[9] A construction involving the use of a hodograph is given by Bourquard ('R. Acad. Sci., Paris,' 1932 loc. cit.) which is equivalent to this result.

p/p_3 derived from (9) are given in Table I and are shown in fig. 2.

The method described above was applied to three cones whose vertical angles are 60°, 40° and 20° (so that $\theta_s = 30°,20°,10°$). In each case a range of values of u_s/c was chosen so as to cover the whole range in which results of interest might be expected. The actual values taken for u_s/c are shown in the top row of each section of Table II while the interval $\delta\theta$ used in the step-by-step integration is given in the second row.

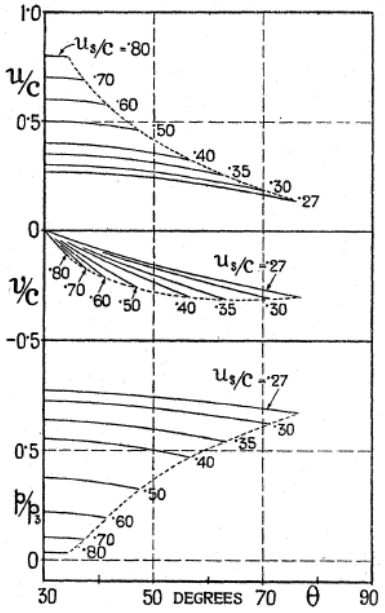

FIG. 2.—u/c, v/c and p/p_3 for 30° cone.

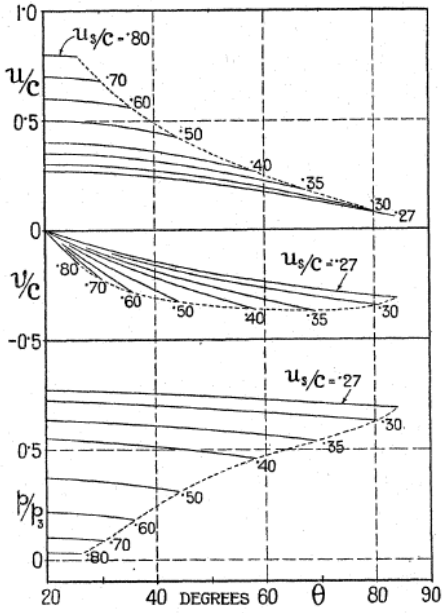

FIG. 3.—u/c, v/c and p/p_3 for 20° cone.

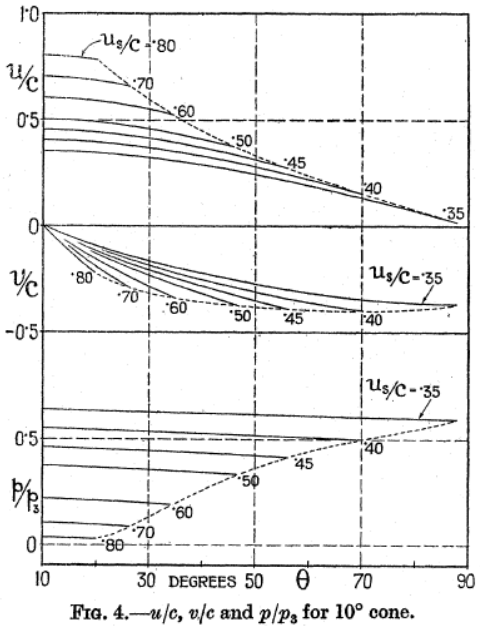

FIG. 4.—u/c, v/c and p/p_3 for 10° cone.

It seems unnecessary to give in tabular form the details of the solutions obtained. They are set forth, however, in graphical form in figs. 2, 3 and 4 where the variations of u/c, v/c and p/p_3 with θ are shown for each

cone, for some, but not all, of the values of u_s / c for which the solutions were obtained.

§4. Shock Wave Equations.

Meyer's equations governing the conditions on either side of an oblique shock wave are (Ackeret, loc. cit., p. 330)

$$\cos^2 \alpha = \left\{ \frac{(\gamma-1)+(\gamma+1)(x/y)}{4\gamma\left[(1/y)^{(\gamma-1)/\gamma}-1\right]} \right\}(\gamma-1), \tag{11}$$

$$\tan\beta = \frac{(\gamma-1)y+(\gamma+1)x}{(\gamma-1)x+(\gamma+1)y}\tan\alpha, \tag{12}$$

where α, β, x, y, γ have the meanings explained in the list of symbols and illustrated in fig. 1.

Our present purpose is to use these equations to find out whether a shock wave is capable of changing the uniform stream at pressure p_1 moving parallel to the axis with velocity U into a stream at pressure p_2 moving at angle $\theta+\phi$ to the axis. For this purpose evidently we must take

$$\pi/2-\alpha=0 \quad \text{and} \quad \beta-\alpha=\theta+\phi. \tag{13}$$

These conditions, however, do not suffice to connect the motion at the two sides of the shock wave. The pressure p/p_3 given by (9) must be equal to p_2/p_3.

But $\frac{p_2}{p_3}=\frac{p_2}{p_0}\frac{p_0}{p_3}=\frac{x}{z}$ so that the pressure condition is

$$\frac{p}{p_3}=\frac{x}{z}. \tag{14}$$

The method adopted for finding the conditions under which (13) and (14) can be satisfied simultaneously was to find for each value of θ and $\theta+\phi$ in the step-by-step calculation the values of x, y and z in the shock wave equations which correspond with values of α and $\beta-\alpha$ given by (13). The values of

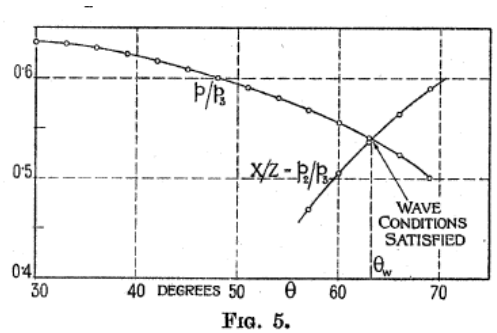

FIG. 5.

p/p_3 obtained in the step-by-step calculation and of x/z were then plotted on a diagram for each value of θ and the point where the two curves cross gives the angle θ_w at which the shock wave can exist so that the required conditions are satisfied. An example of this kind of diagram is shown in fig. 5.

In his presentation of the shock wave equations, Meyer calculated the values of α and β from (11) and (12) for a limited number of values of x and y. He then plotted on an x, y diagram three sets of interpolated curves showing the values of x and y for a limited number of values of α, β and $\beta - \alpha$, respectively. To find x and y for given values of α and $\beta - \alpha$ two of these diagrams would have to be superimposed and the co-ordinates of the intersections of the corresponding contours read. This method turns out to involve considerable difficulties in interpolation; accordingly, two new sets of curves were plotted with α and $\beta - \alpha$ as rectangular co-ordinates. One of these, fig. 6, gives the value of x corresponding with any given values of α and $\beta - \alpha$, the other, fig. 7, gives the value of y.[10] Most of the values of x and

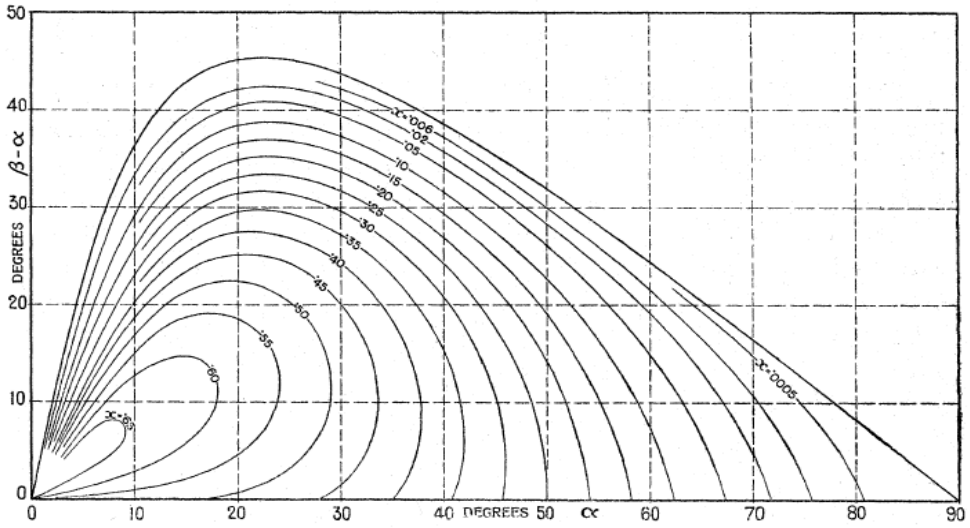

FIG. 6.

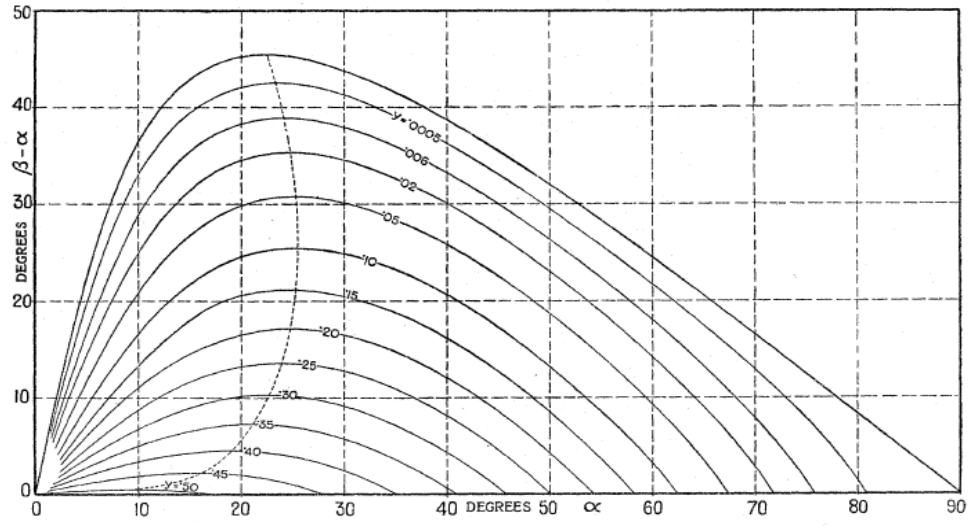

FIG. 7.

[10] It will be noticed from (12) that the limiting forms of these contours when $x = 0$ or when $y = 0$ are identical, namely, $\tan\beta = \frac{\gamma+1}{\gamma-1}\tan\alpha$.

y in Table II were found in this way, though in some cases when the points occurred near the limits of the diagram direct calculation was used, (11) and (12) being solved as simultaneous equations in x and y for appropriate values of α and $\beta - \alpha$.

Meyer's equations do not give z directly. This can be obtained by constructing the equation for β which is analogous to the expression (11) giving α in terms of y and x/y. For this purpose it is merely necessary to substitute in (11) β for α, y/x for x/y, and z/x for $1/y$.[11]

$$\cos^2\beta = \left\{\frac{(\gamma-1)+(\gamma+1)y/x}{4\gamma[(z/x)^{(\gamma-1)/\gamma}-1]}\right\}(\gamma-1)$$

The resulting equation can be re-arranged into the form

$$\left(\frac{z}{x}\right)^{\frac{\gamma-1}{\gamma}} = 1 + \frac{\gamma-1}{4\gamma\cos^2\beta}\left\{\gamma - 1 + (\gamma+1)\frac{y}{x}\right\}. \qquad (15)$$

After the tables for α and β, from which figs. 6 and 7 were prepared, had been made they were used in conjunction with (15) to construct a table giving z in terms of x and y. The diagram of fig. 8 shows how z varies with. x for constant values of y.

It will be noticed that this diagram is contained within a certain **bounding curve** which corresponds with $\alpha = \beta = 0$. The x and z co-ordinates of this curve were calculated separately for various values of y so as to check the calculations. The formulae used for this purpose were derived by putting $\cos\alpha = \cos\beta = 1$ in (11) and (15). They are

$$\frac{x}{y} = \frac{1}{\gamma^2-1}\left[4\gamma y^{\frac{1-\gamma}{\gamma}} - (\gamma+1)^2\right]$$

and

$$\left(\frac{z}{x}\right)^{\frac{\gamma-1}{\gamma}} = 1 + \frac{(\gamma-1)^2}{4\gamma} + \frac{(\gamma^2-1)^2}{16\gamma^2\left(y^{\frac{1-\gamma}{\gamma}} - \frac{(\gamma+1)^2}{4\gamma}\right)}.$$

The values of x and y derived from figs. 6 and 7 and entered in Table I were used in conjunction with fig. 8 to find the values of z given near the foot of the table. The values of x/z found in this way are plotted in fig. 5 as a function of θ.

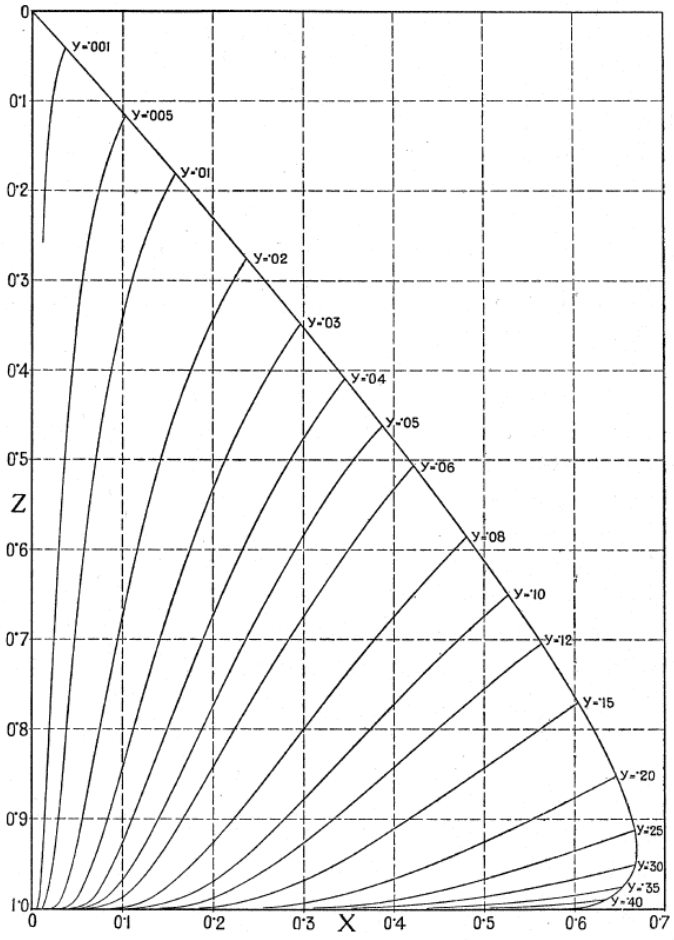

Fig. 8.

[11] I.e., p_2/p_3 for p_1/p_0.

The position of the shock wave is determined by the intersection of the curves for *x*/*z* and p/p_3. In the particular case $\theta_s = 30°$, $u_s/c = 0.35$ which is shown in fig. 5 the intersection occurs at $\theta = 63.3°$, and this value is entered as θ_w in Table II.

The same process was repeated for each of the other initial conditions, and the results set forth in Table II.

Graphical Representation of Solutions.-To gain a clearer understanding of the manner in which the various physical quantities occurring in the solution depend on the speed and vertical angle of the cones, the values of *x*, *y* and *z* have been plotted as functions of u_s/c for each of the cones. The resulting curves are shown in figs. 9, 10 and 11.

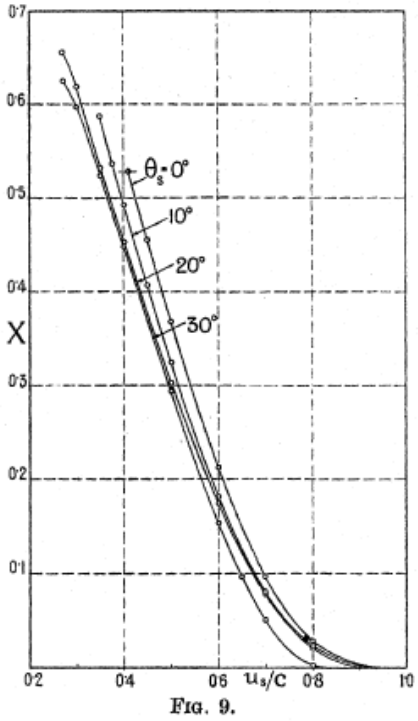

FIG. 9.

In the limiting case of a cone of very **small vertical angle**, i.e., when $\theta_s \to 0$ the disturbance is very small so that $U = u_s$, $x = y$, $c = c_1$ and $z = 1$. The relation (10A) thus becomes

$$x = y = \left[1 - \left(\frac{u_s}{c}\right)^2\right]^{\frac{\gamma}{\gamma-1}}. \qquad (16)$$

The limiting curves for $\theta_s = 0$ are plotted in figs. 9 and 10 by means of equation (16).

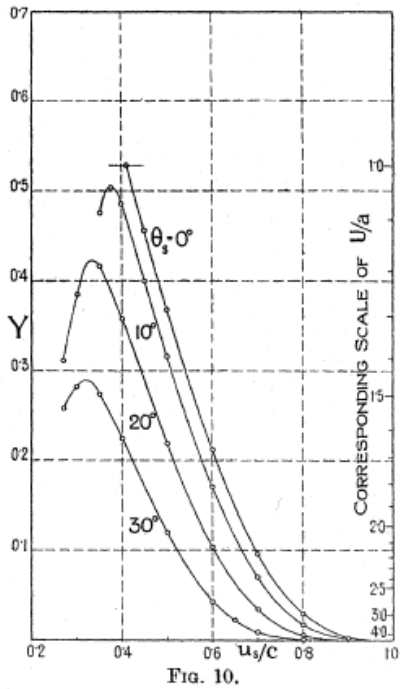

FIG. 10.

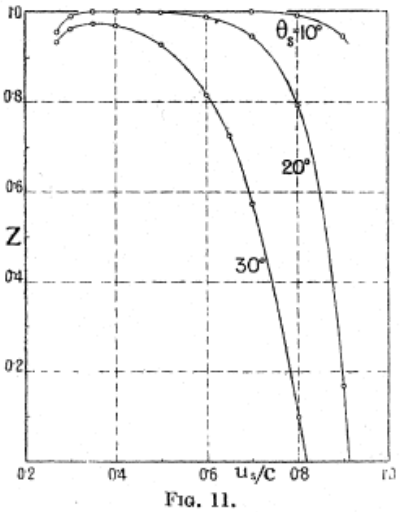

FIG. 11.

§5. Reduction of Results to Familiar Forms.

It remains to reduce the results summarised in Table II to a form convenient for comparison with observation. The velocity of the undisturbed stream (corresponding with the speed of a bullet when considered relative to still air) is found by inserting the value of y given in Table II in equation (10B). The values of U/a so found are also given in Table II.

The pressure at any point is derivable from the values for p/p_3 given by (9). In this form, however, it is not available for comparison with experimental results which are usually given in the form $\frac{p-p_1}{\rho_1 U^2}$. This is connected with p/p_3 by means of the formula

$$\frac{p-p_1}{\rho_1 U^2} = \left(\frac{pz}{p_3 y} - 1\right) \cdot \frac{a^2}{\gamma U^2}. \qquad (17)$$

The physical quantity which can most easily be measured is p_s the pressure at the surface of the cone. The calculated values of $\frac{p_s - p_1}{\rho_1 U^2}$ are given in Table II and are shown as functions of U/a in fig. 12.

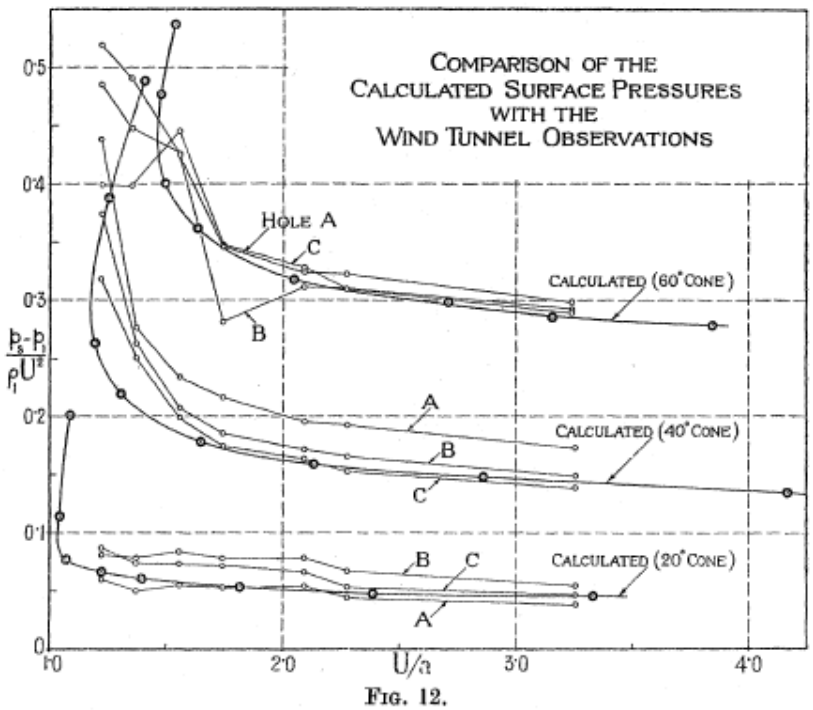

FIG. 12.

Another physical quantity that can be measured is θ_w. This is the angle which the shock wave makes with the axis of a pointed bullet at its point. It can be measured in a bullet photograph which shows the wave of compression. θ_w has, therefore, been plotted in fig. 13 as a function of U/a for each of the three cones.

The limiting value of θ_w when $\theta_s \to 0$ is evidently the Mach angle $\sin^{-1}\frac{a}{U}$, so that the equation to the limiting curve for $\theta_s = 0$ is $\frac{U}{a} = \operatorname{cosec}\theta_w$. This is plotted as a broken line in fig. 13.

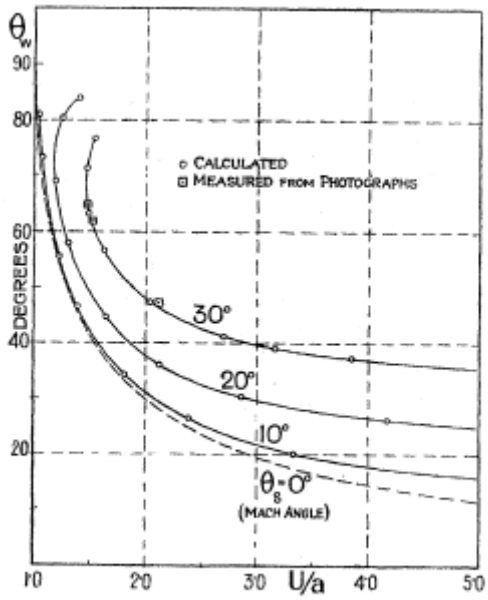

FIG. 13.

A point which seems worth noticing in connection with these solutions is that in some of them the speed of flow behind the shock wave is everywhere lower than the local speed of sound. In some it is everywhere higher. In the remaining cases the speed of flow is greater than that of sound immediately behind the shock wave, but it decreases till at the surface of the cone it is less than that of sound. In these cases the speed of flow is equal to the local speed of sound at some value θ_a which is intermediate between θ_w and θ_s. The various cases are distinguished in Table II and the values of θ_a are given when this symbol has a physical meaning.

The ratio of the speed to the local speed of sound is a function of p/p_3 only. If q represents the speed while a^* is the local speed of sound at a point where the velocity is q

$$\left(\frac{q}{a^*}\right)^2 = \frac{2}{\gamma-1}\left[\left(\frac{p_3}{p}\right)^{\frac{\gamma-1}{\gamma}} - 1\right], \qquad (18)$$

so that $q = a^*$ when $\left(\frac{p_3}{p}\right)^{\frac{\gamma-1}{\gamma}} = \frac{\gamma+1}{2}$. Under these conditions

$$\frac{q}{c} = \sqrt{\frac{\gamma-1}{\gamma+1}} = 0.41\,. \qquad (19)$$

Since the minimum velocity occurs at the surface of the solid cone this implies that if $u_s / c > 0.41$ the speed is everywhere greater than that of sound. In the case of the 60° cone (it can be seen in fig. 10) $u_s / c = 0.41$ corresponds with $U/a = 1.66$.

When the speed of flow exceeds the local speed of sound stationary wavelets can exist at angle $M = \sin^{-1} \frac{a^*}{q}$ to the stream lines. This angle which might be called the "local Mach angle" has been calculated in some cases for which the streamlines have been drawn, and the actual forms which stationary wavelets would assume have been drawn as dotted lines in fig. 14. In the case of the 60° cone it is only when $U/a > 1.66$ that the region for which $q > a^*$ extends to the surface, so that it is only when $U/a > 1.66$ that stationary wavelets are likely to be produced by irregularities on the surface of the solid cone.

Streamlines.-To trace the streamlines the angle $\phi = \tan^{-1} \frac{v}{u}$ is found for each value of θ and the direction of the element of streamline between θ and $\theta + \delta\theta$ is traced. Beginning at some point on the shock wave the streamline is traced till it becomes so nearly parallel to the cone that it runs out of the portion of the field under consideration. Streamlines traced in this way are shown in fig. 14.

§6. Limitations to the Application of the Solutions.

The curves of fig. 12 which give the variations of $\frac{p_s - p_1}{\rho_1 U^2}$ - with U/a reveal a remarkable limitation to the applicability of the conical solution. As U/a decreases from large values, $\frac{p_s - p_1}{\rho_1 U^2}$ gradually rises till at some critical value, namely, $U/a = 1.46$ for the 60° cone, 1.18 for the 40° cone and 1.035 for the 20° cone, a minimum possible value of U/a is reached. At speeds lower than this critical speed the conical regime cannot exist. If U/a is determined as it is in the case of a projectile with a conical head, moving at a given speed (greater than the critical speed), there are two mathematically possible regimes, one corresponding with the lower part of the curve of fig. 12 and one corresponding with the upper part. It seems unlikely that the second regime corresponding with the higher surface pressure would be realised under experimental conditions in front of a cylindrical body with a simple conical head.

The nature of regimes which could exist near the conical nose of a projectile

moving at less than the critical speed into still air is discussed later in connection with photographs of bullets.

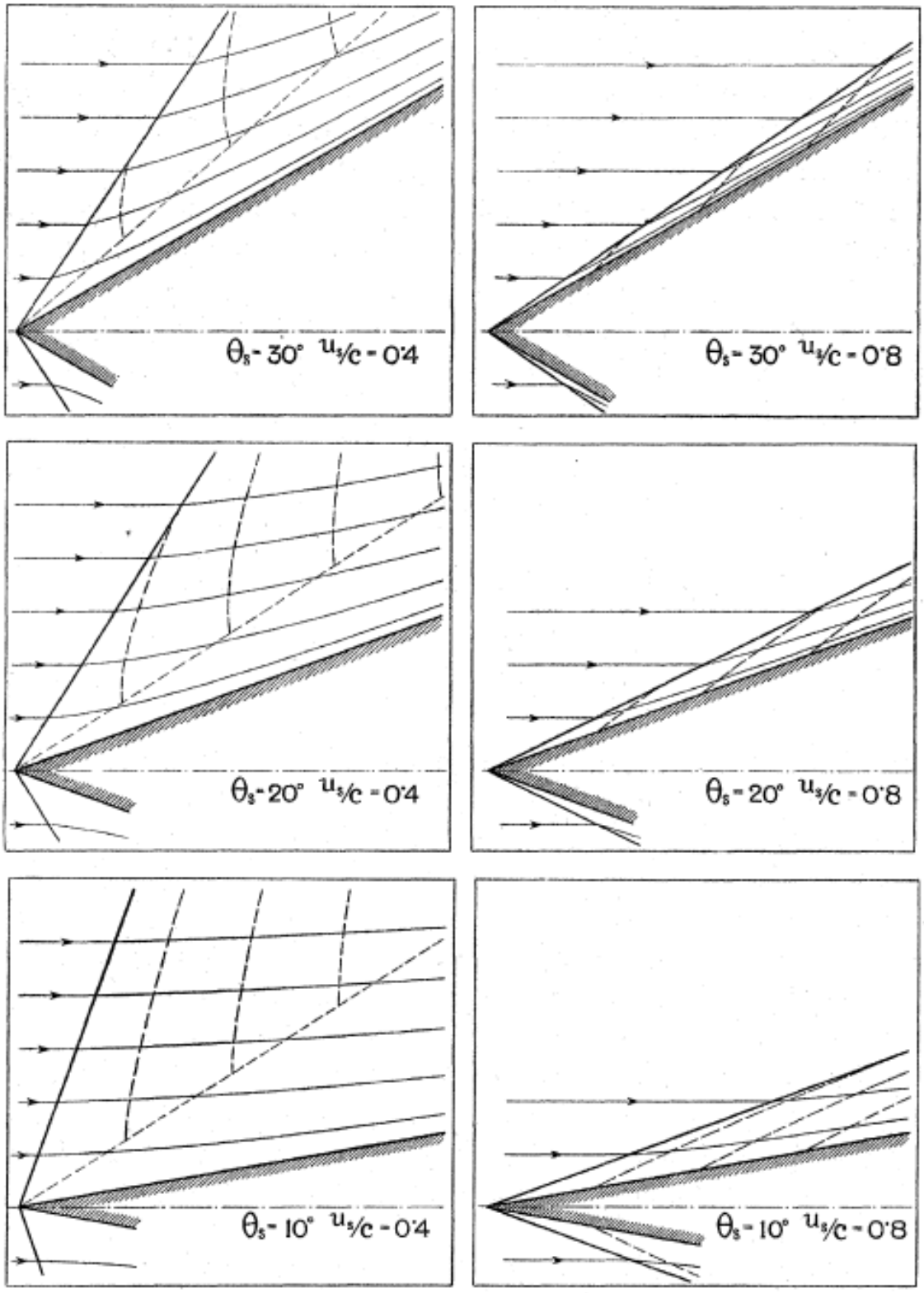

FIG. 14.

Table I.—Abridged Form of the Calculations for $\theta_s = 30°$, $u_s/c = 0{\cdot}35$.

$v_\theta/c = c^{-1} \,.\, [du/d\theta]_\theta \qquad = c^{-1} \,.\, \{v_{\theta-\delta\theta} + \delta\theta \,.\, [d^2u/d\theta^2]_{\theta-\delta\theta}\}$

$u_\theta/c = c^{-1} \,.\, \{u_{\theta-\delta\theta} + \delta\theta \,.\, [v_M]\}, \qquad$ where $v_M = \frac{1}{2}\{v_\theta + v_{\theta-\delta\theta}\}$

$-c^{-1} \,.\, d^2u/d\theta^2 = L/M, \qquad$ where $L = c^{-3} \,.\, [0{\cdot}405\,\{c^2 - u^2 - v^2\}\{u + \frac{1}{2}v \,.\, \cot\theta\} - uv$

and $M = c^{-2} \,.\, [0{\cdot}2025\,(c^2 - u^2) - 1{\cdot}2025\,v^2]$

$p/p_3 = [c^{-2} \,.\, (c^2 - u^2 - v^2)]^{3{\cdot}469}$

$\tan\phi = v/u \qquad \beta - \alpha = \theta + \phi \qquad \alpha = \pi/2 - \theta.$

θ °.	30.	33.	36.	39.	42.	45.	48.
$-v/c$	0·0000	0·03665	0·07036	0·10192	0·13182	0·16039	0·18784
u/c	0·3500	0·34904	0·34624	0·34173	0·33561	0·32796	0·31884
$c^{-2} \,.\, [c^2 - u^2 - v^2]$	0·8775	0·87683	0·87517	0·87283	0·86999	0·86672	0·86306
$c^{-1} \,.\, [u + \frac{1}{2}v \,.\, \cot\theta]$	0·3500	0·32082	0·29782	0·27880	0·26241	0·24776	0·23427
L	0·12439	0·11346	0·10385	0·09500	0·08663	0·07853	0·07064
M	0·17769	0·17622	0·17227	0·16636	0·15879	0·14979	0·13948
$-c^{-1} \,.\, d^2u/d\theta^2$	0·7000	0·6439	0·6028	0·5711	0·5456	0·5243	0·5065
p/p_3	0·6355	0·6338	0·6297	0·6239	0·6168	0·6088	0·6000

θ.	51.	54.	57.	60.	63.	66.	69.
$-v/c$	0·21436	0·24009	0·26518	0·28984	0·31433	0·33920	0·36562
u/c	0·30831	0·29641	0·28318	0·26865	0·25283	0·23572	0·21727
$c^{-2} \,.\, [c^2 - u^2 - v^2]$	0·85899	0·85450	0·84949	0·84382	0·83728	0·82938	0·81911
$c^{-1} \,.\, [u + \frac{1}{2}v \,.\, \cot\theta]$	0·22152	0·20919	0·19708	0·18498	0·17275	0·16021	0·14710
L	0·06289	0·05530	0·04789	0·04064	0·03360	0·02669	0·01975
M	0·12799	0·11539	0·10170	0·08687	0·07075	0·05289	0·03219
$-c^{-1} \,.\, d^2u/d\theta^2$	0·4914	0·4792	0·4709	0·4678	0·4749	0·5046	0·6135
p/p_3	0·5902	0·5796	0·5679	0·5548	0·5400	0·5226	0·5003
$-\tan\phi$			0·9364	1·0789	1·2432	1·4390	1·6828
$-\phi$			43° 07′	47° 10′	51° 11′	55° 12′	59° 17′
Shock wave conditions: $\beta - \alpha$			13° 53′	12° 50′	11° 49′	10° 48′	9° 43′
Shock wave conditions: α			33° 00′	30° 00′	27° 00′	24° 00′	21° 00′
Shock wave conditions: x			0·452	0·489	0·521	0·550	0·574
Shock wave conditions: y			0·221	0·248	0·272	0·291	0·308
Shock wave conditions: z			0·964	0·969	0·972	0·975	0·975
$p_2/p_3 = x/z$			0·469	0·505	0·536	0·564	0·589

Table II.—Summary of Results of Calculations.

$\theta_s = 10°$.

u_s/c.	0·35.	0·375.	0·40.	0·45.	0·50.	0·60.	0·70.	0·80.	0·90.
$\delta\theta$	3·0°	2·0°	2·0°	1·5°	1·5°	1·5°	1·0°	0·5°	0·5°
x	0·587	0·536	0·493	0·408	0·325	0·182	0·0802	0·0236	0·00263
y	0·476	0·504	0·486	0·401	0·316	0·171	0·0700	0·0168	0·00115
z	0·999	1·000	1·000	1·000	1·000	1·000	1·000	0·992	0·946
θ_w	87·9°	81·1°	70·3°	55·6°	46·6°	34·4°	26·3°	20·1°	15·4°
U/a	1·09	1·04	1·07	1·22	1·39	1·81	2·39	3·33	5·46
Mach angle	67·1°	74·3°	69·3°	55·0°	45·8°	33·5°	24·8°	17·5°	10·6°
θ_a	*	*	32·5°	†	†	†	†	†	†
$(p_s - p_1)/\rho_1 U^2$	0·202	0·114	0·077	0·066	0·060	0·054	0·048	0·045	0·038

$\theta_s = 20°$.

u_s/c.	0·27.	0·30.	0·35.	0·40.	0·50.	0·60.	0·70.	0·80.	0·90.
$\delta\theta$	3·0°	3·0°	3·0°	2·0°	1·5°	1·5°	1·0°	0·5°	0·5°
x	0·656	0·619	0·532	0·453	0·303	0·175	0·0781	0·0203	$0·502\times10^{-3}$
y	0·312	0·385	0·417	0·358	0·219	0·104	0·0339	0·00534	$0·295\times10^{-4}$
z	0·954	0·989	0·999	0·999	0·998	0·987	0·945	0·791	0·170
θ_w	84·1°	80·4°	69·1°	58·0°	44·4°	36·1°	30·4°	26·2°	22·9°
U/a	1·40	1·25	1·19	1·30	1·65	2·13	2·86	4·17	9·74
Mach angle	45·4°	53·1°	57·1°	50·1°	37·4°	28·0°	20·5°	13·9°	5·9°
θ_a	*	*	*	32·7°	†	†	†	†	†
$(p_s - p_1)/\rho_1 U^2$	0·488	0·388	0·263	0·219	0·178	0·159	0·148	0·134	0·128

$\theta_s = 30°$.

$u_s/_1c$.	0·27.	0·30.	0·35.	0·40.	0·50.	0·60.	0·65.	0·70.	0·80.
$\delta\theta$	3·0°	3·0°	3·0°	2·0°	1·0°	1·0°	1·0°	1·0°	0·5°
x	0·625	0·597	0·524	0·448	0·294	0·154	0·0968	0·0506	$0·271\times10^{-2}$
y	0·258	0·282	0·274	0·224	0·119	0·0424	0·0216	0·0082	$0·122\times10^{-3}$
z	0·933	0·961	0·972	0·967	0·926	0·815	0·725	0·574	0·0997
θ_w	76·8°	71·4°	63·3°	56·6°	47·4°	41·3°	39·2°	37·3°	34·2°
U/a	1·54	1·47	1·49	1·63	2·05	2·71	3·16	3·85	7·84
Mach angle	40·6°	42·7°	42·1°	37·8°	29·3°	21·7°	18·5°	15·1°	7·3°
θ_a	*	*	*	41·0°	†	†	†	†	†
$(p_s - p_1)/\rho_1 U^2$	0·537	0·477	0·401	0·362	0·318	0·299	0·285	0·278	0·262

* Speeds behind the shock wave everywhere less than that of sound.
† Speeds behind the shock wave everywhere greater than that of sound.

Reader's exercise.

A. Drawing Figure 7.

Drawing Figure 7 is rather simple. This essentially a graph of α vs. β with a parameter y (eliminating x).

$$\cos^2\alpha = \left\{\frac{(\gamma-1)+(\gamma+1)(x/y)}{4\gamma\left[(1/y)^{(\gamma-1)/\gamma}-1\right]}\right\}(\gamma-1), \tag{11}$$

$$\tan\beta = \frac{(\gamma-1)y+(\gamma+1)x}{(\gamma-1)x+(\gamma+1)y}\tan\alpha, \tag{12}$$

From Eq. (12) we have

$$\frac{x}{y} = \frac{(\gamma-1)\tan\alpha-(\gamma+1)\tan\beta}{(\gamma-1)\tan\beta-(\gamma+1)\tan\alpha}. \tag{A1}$$

Eq. (11) has an *x*/*y* term. So we use this relation. We solve Eq. (11) for *x*

$$\frac{4\gamma[(1/y)^{(\gamma-1)/\gamma}-1]}{\gamma-1}\cos^2\alpha = (\gamma-1)+(\gamma+1)\frac{x}{y} \tag{A2}$$

$$x = \left\{\frac{4\gamma[(1/y)^{(\gamma-1)/\gamma}-1]}{\gamma-1}\cos^2\alpha-(\gamma-1)\right\}\frac{y}{\gamma+1}. \tag{A3}$$

Substituting (A3) into Eq. (12) we have α vs. β relation with a parameter y. The graph is as follows.

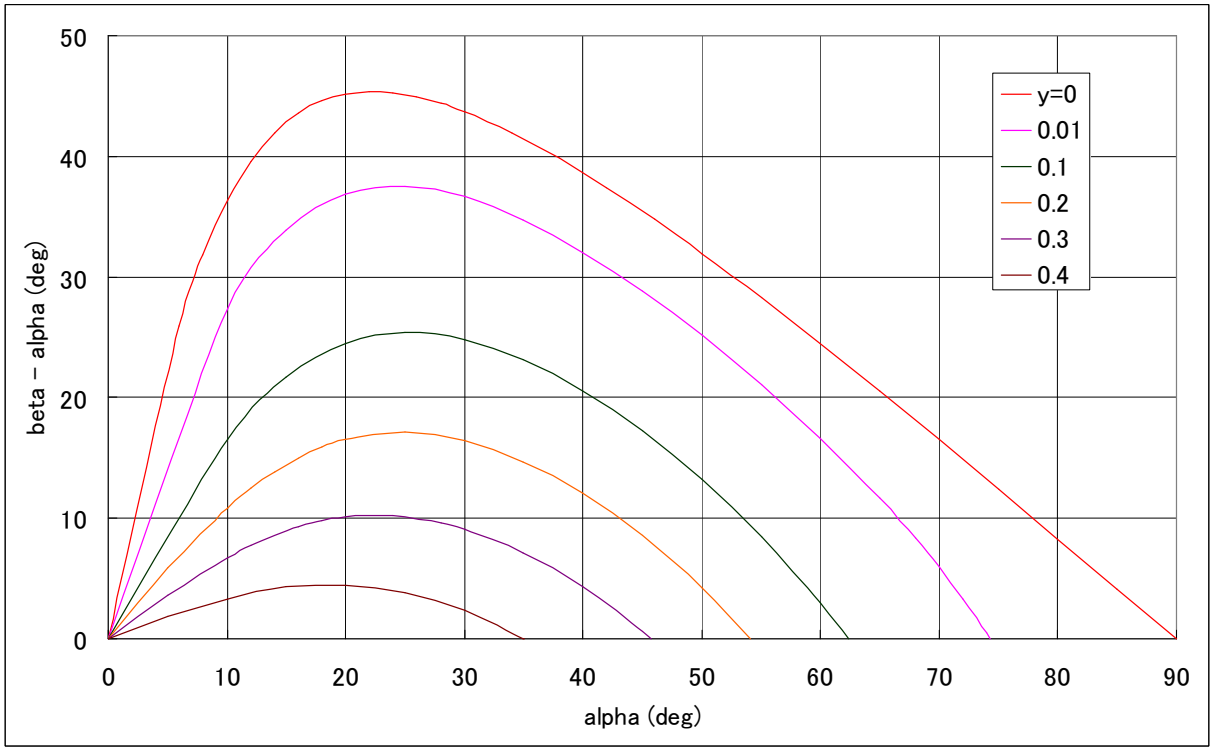

For each y there is a maximum for x. This is shown in the following figure.

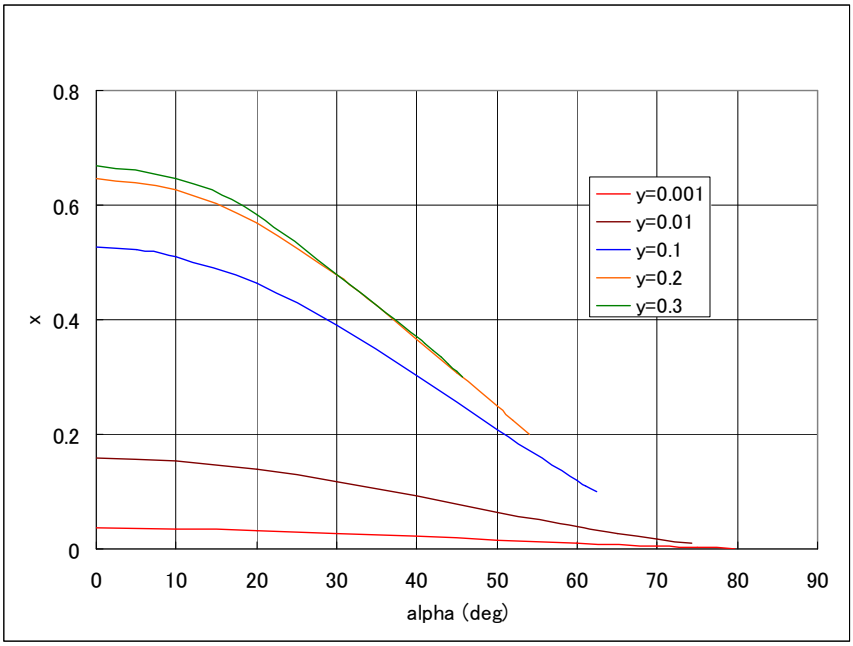

B. Drawing Figure 6.

Figure 6 is a graph of α vs. β with a parameter x. We need to eliminate y in the process. In eliminating y we need some iteration to solve y.

Eq. (A2) is

$$\frac{4\gamma[(1/y)^{(\gamma-1)/\gamma}-1]}{\gamma-1}\cos^2\alpha=(\gamma-1)+(\gamma+1)\frac{x}{y}. \qquad \text{(A2)}$$

We put $Y = 1/y$ and rearrange (A2) as follows.

$$F(Y)=\frac{4\gamma}{\gamma-1}\cos^2\alpha Y^{(\gamma-1)/\gamma}-(\gamma+1)xY-\frac{4\gamma}{\gamma-1}\cos^2\alpha-(\gamma-1).$$

To get Y for $F(Y) = 0$ we use Newton method. That is

$$Y_{i+1}=Y_i-\frac{F_i}{F'_i},$$

where

$$F'(Y)=4\cos^2\alpha Y^{-1/\gamma}-(\gamma+1)x.$$

A few times of iteration gives a solution of Y with a good accuracy.

In giving an initial value of Y we have to take care of the fact that in a certain range of x there are two solutions of $F(Y)$=0. This is shown as follows.

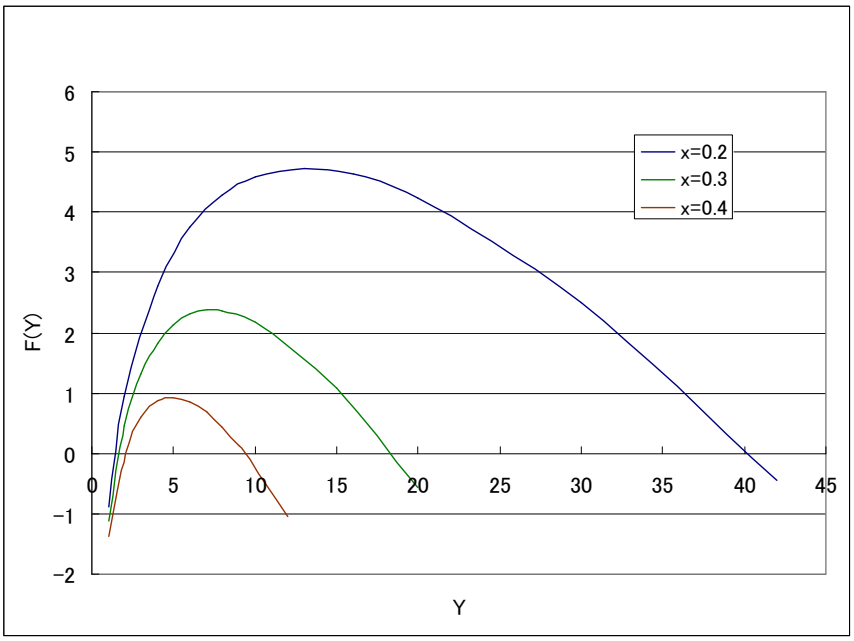

The final graph for α vs. β with a parameter x is as follows.

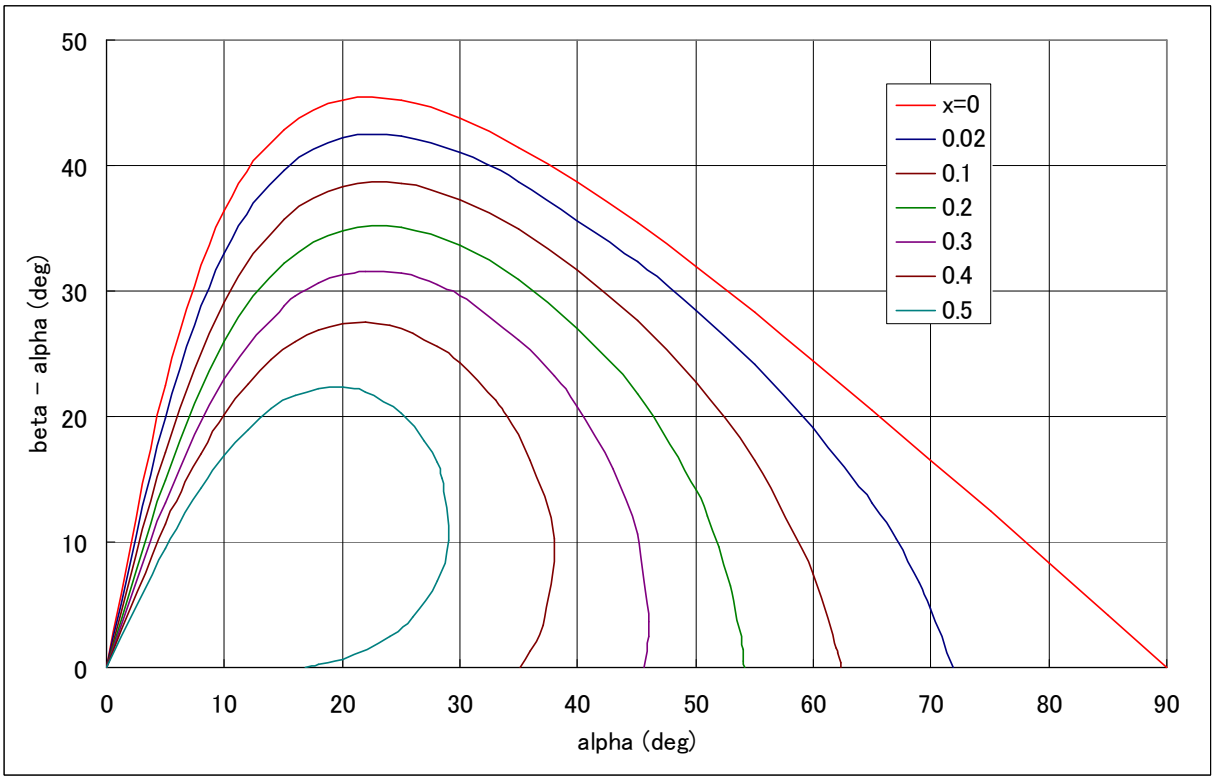

C. Overlapping plot of Figures 6 and 7.

The overlapping plot of these figures is as follows.

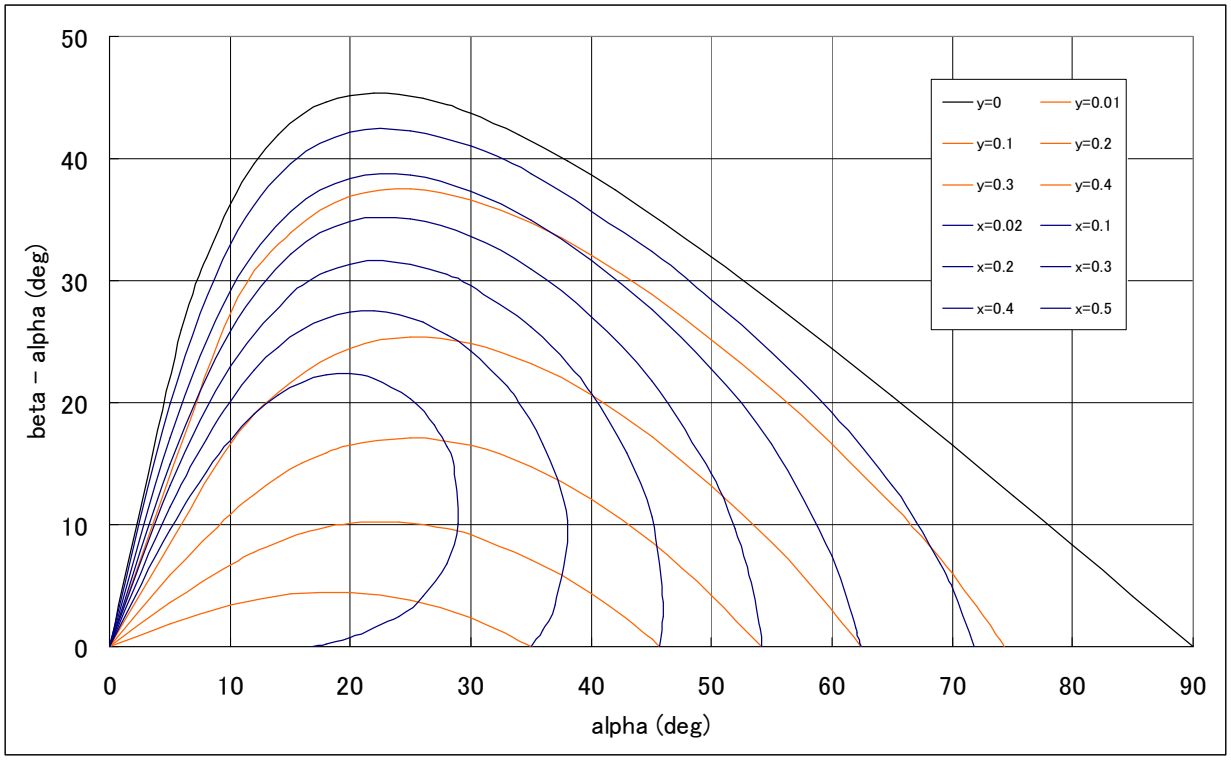

D. Getting the values of *x*, *y* and *z*.

The exact values of *x* and *y* are obtained by the iteration procedure of solving Eq. (11) and (12). An example of the iteration is as follows.

(1) Assume a proper value of y.

(2) Get *x* from Eq. (A3).

$$x = \left\{ \frac{4\gamma[(1/y)^{(\gamma-1)/\gamma} - 1]}{\gamma - 1} \cos^2\alpha - (\gamma - 1) \right\} \frac{y}{\gamma + 1} . \qquad \text{(A3)}$$

(3) Get *y* from Eq. (A1) or

$$y = \frac{(\gamma - 1)\tan\beta - (\gamma + 1)\tan\alpha}{(\gamma - 1)\tan\alpha - (\gamma + 1)\tan\beta} x .$$

(4) Return to step (2) to get *x* and repeat the procedure.

(5) Continue a few steps to get the solution of enough accuracy.

The value of *z* is given by Eq. (15) or

$$z = x\left\{ 1 + \frac{\gamma - 1}{4\gamma} \frac{1}{\cos^2\alpha} \left[(\gamma - 1) + (\gamma + 1)\frac{y}{x} \right] \right\}^{\gamma/(\gamma-1)} .$$